ACS OMEGA

http://pubs.acs.org/journal/acsodf

Article

Integrating UPLC-HR-MS/MS, Network Pharmacology, and Experimental Validation to Uncover the Mechanisms of Jin'gan Capsules against Breast Cancer

Jianfei Qiu, Zhiyin Zhang, Anling Hu, Peng Zhao, Xuenai Wei, Hui Song,* Jue Yang,* and Yanmei Li*

Cite This: *ACS Omega* 2022, 7, 28003−28015

Read Online

ACCESS | Metrics & More | Article Recommendations | Supporting Information

ABSTRACT: In the theory of traditional Chinese medicine (TCM), "liver-qi" stagnation and heat-induced toxicity represent the main etiologies of breast cancer. Recently, several TCMs with heat-clearing and detoxification efficacy have shown inhibitory effects on breast cancer. Jin'gan capsules (JGCs), initially approved to treat colds in China, are a heat-clearing and detoxification TCM formula. However, the anticancer activity of JGCs against breast cancer and its underlying mechanisms remain unclear. First, we assessed the antiproliferative activity of JGCs in breast cancer cell lines and evaluated their effects on cell apoptosis and the cell cycle by flow cytometry. Furthermore, we identified the potential bioactive components of JGCs and their corresponding target genes and constructed a bioactive compound−target interaction network by ultra-performance liquid chromatography−high-resolution tandem mass spectrometry (UPLC-HR-MS/MS) and network pharmacology analysis. Finally, the underlying mechanism was investigated through gene function enrichment analysis and experimental validation. We found that JGCs significantly inhibited breast cancer cell growth with IC_{50} values of 0.56 ± 0.03, 0.16 ± 0.03, and 0.94 ± 0.09 mg/mL for MDA-MB-231, MDA-MB-468, and MCF-7, respectively. In addition, JGC treatment dramatically induced apoptosis and S phase cell cycle arrest in breast cancer cells. Western blot analysis confirmed that JGCs could regulate the protein levels of apoptosis- and cell cycle-related genes. Utilizing UPLC-HR-MS/MS analysis and network pharmacology, we identified 7 potential bioactive ingredients in JGCs and 116 antibreast cancer targets. Functional enrichment analysis indicated that the antitumor effects of JGCs were strongly associated with apoptosis and the Janus kinase (JAK)-signal transducer and activator of transcription (STAT) signaling pathway. Western blot analysis validated that JGC treatment markedly decreased the expression levels of *p*-JAK2, *p*-STAT3, and STAT3. Our findings suggest that JGCs suppress breast cancer cell proliferation and induce cell cycle arrest and apoptosis partly by inhibiting the JAK2/STAT3 signaling pathway, highlighting JGCs as a potential therapeutic candidate against breast cancer.

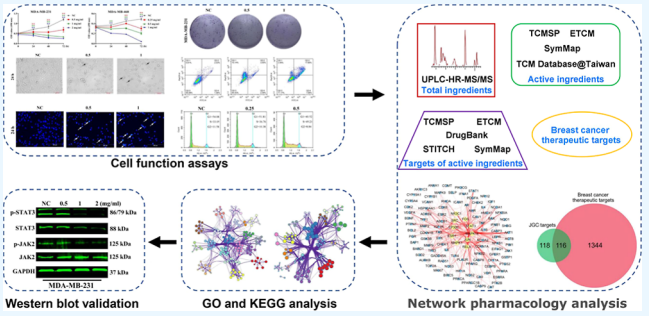

1. INTRODUCTION

In 2020, for the first time, the incidence of female breast cancer exceeded that of lung cancer as the most common cancer worldwide.[1] Although progress has been made regarding diagnostic and therapeutic strategies, including surgery, chemotherapy, endocrine therapy, targeted therapy, and immunotherapy, the prognosis of patients diagnosed with breast cancer remains unsatisfactory.[2,3] Notably, triple-negative breast cancer (TNBC) is considered to be the most incurable and refractory subtype due to the aberrant expression of the estrogen receptor (ER), progesterone receptor, and human epidermal growth factor receptor 2.[4] In addition, long-term chemotherapy has many side effects and will eventually increase the risk of developing drug resistance. The problems mentioned above have seriously hampered the successful treatment of breast cancer, and therefore, it is urgent to establish new therapeutic strategies.

In the theory of traditional Chinese medicine (TCM), the main etiologies of breast cancer are "liver-qi" stagnation, heat-induced toxicity, and phlegm accumulation.[5,6] Accordingly, several TCMs with heat-clearing and detoxification efficacy show certain curative effects on breast cancer. For instance, Shuganning injection inhibits tumor growth and promotes cell ferroptosis in TNBC.[7] Qingdu granules were reported to suppress tumor growth and breast cancer cell angiogenesis by regulating the nuclear factor of activated T-cell (NFAT) pathway.[8] Xi huang pills inhibited the growth of breast cancer in vitro and in vivo.[9] The abovementioned studies support the

Received: March 29, 2022
Accepted: July 25, 2022
Published: August 7, 2022

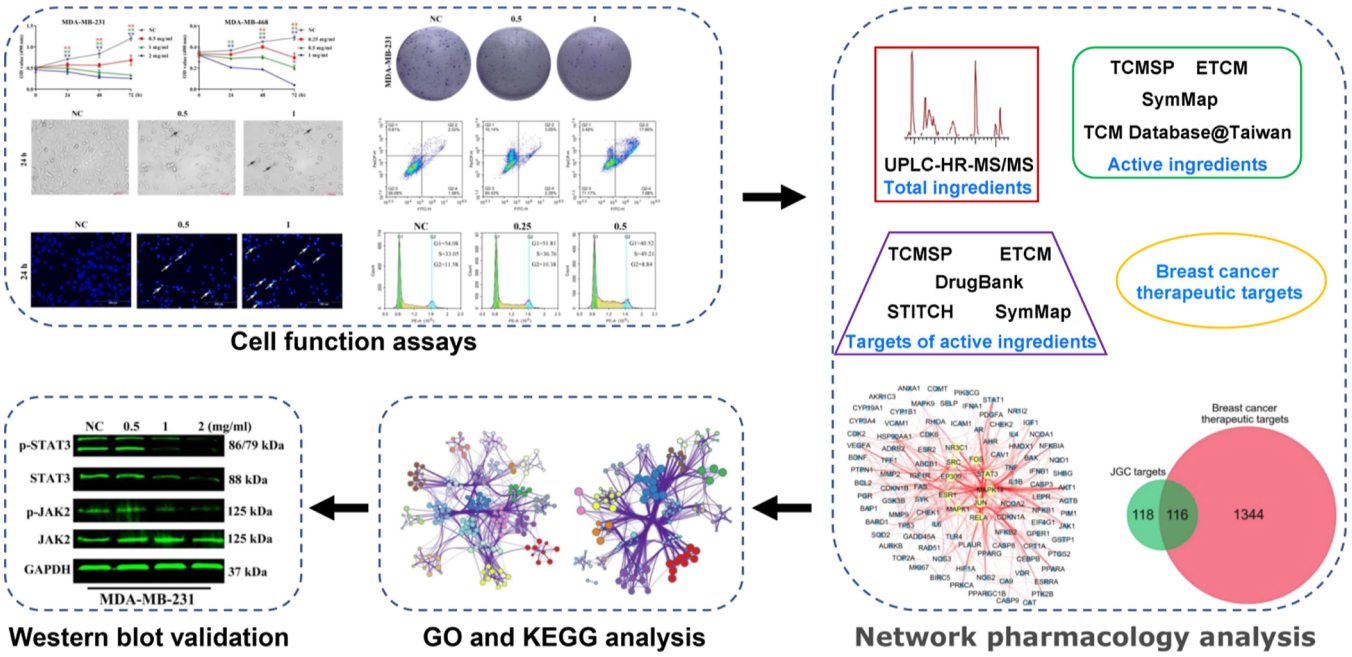

Figure 1. Integrated workflow of the network pharmacology and experimental studies of JGCs against breast cancer.

notion that heat-clearing and detoxifying TCMs have great potential for breast cancer treatment. Therefore, identifying drugs from this kind of TCM with antibreast cancer activity and understanding the molecular mechanism might provide new alternative therapies for breast cancer treatment.

Jin'gan capsules (JGCs), a heat-clearing and detoxifying formula in Miao medicine, were approved to treat colds (such as fever, headache, cough, and sore throat) in the clinic by the China Food and Drug Administration (no. Z20059013) in 2005. JGC treatment has the potential to cause side effects, including drowsiness, fatigue, thirst, rash, urticaria, and granulocytopenia. Additionally, the long-term use of large amounts of this drug may increase the risk of liver and kidney dysfunction. However, these symptoms can be relieved automatically after drug withdrawal. According to the etiology of breast cancer in TCM theory, JGCs, with the effects of heat-clearing and detoxification, might have the potential to treat breast cancer. However, their antibreast cancer activity remains unknown.

JGCs are composed of seven botanical drugs, including *Lonicera japonica* Thunb. [Caprifoliaceae; *L. japonicae* flos], *Andrographis paniculata* (Burm.f.) Nees [Acanthaceae; Andrographis herba], *Isatis tinctoria* L. [Brassicaceae; Isatidis radix], *Taraxacum mongolicum* Hand.-Mazz. [Compositae; Taraxaci herba], acetaminophen, amantadine hydrochloride, and chlorphenamine maleate. Previous studies have demonstrated that some extracts from the five botanical drugs in JGCs, including *L. japonica* Thunb.,[10,11] *A. paniculata* (Burm.f.) Nees,[12,13] *I. tinctoria* L.,[14] *T. mongolicum* Hand.-Mazz.,[15,16] and acetaminophen,[17] suppressed the malignant phenotype of breast cancer.

The present study aimed to explore the antibreast cancer activity of JGCs and the molecular mechanism. First, we assessed the antiproliferative activity of JGCs in breast cancer cell lines. Then, we evaluated the effects of JGCs on cell apoptosis and the cell cycle by flow cytometry. Furthermore, we identified the potential bioactive components of JGCs and their corresponding target genes and constructed a bioactive compound−target interaction network by ultra-performance liquid chromatography−high-resolution tandem mass spectrometry (UPLC-HR-MS/MS) and network pharmacology analysis. Finally, the underlying mechanism was investigated through gene function enrichment analysis and experimental validation (Figure 1).

2. RESULTS

2.1. JGCs Inhibited Breast Cancer Cell Viability and Proliferation. Three breast cancer cell lines were employed to evaluate the effect of JGCs on cell viability and proliferation. As shown in Figure 2a, JGCs clearly inhibited the viability of all cell lines in a concentration-dependent manner. Notably, two TNBC cell lines, MDA-MB-231 and MDA-MB-468, were more sensitive to JGCs, with IC_{50} values of 0.56 ± 0.03 and 0.16 ± 0.03 mg/mL, respectively, after 72 h of incubation than the non-TNBC breast cancer cell line MCF-7 (IC_{50} = 0.94 ± 0.09 mg/mL). The proliferation ability was further evaluated by constructing cell growth curves and performing colony formation assays. As shown in Figure 2b−d, JGCs inhibited the proliferation of MDA-MB-231 and MDA-MB-468 cells in a time- and concentration-dependent manner. Moreover, after treatment with different doses of JGCs for 24 and 48 h, MDA-MB-231 and MDA-MB-468 cells exhibited apoptotic morphologies as observed by inverted microscopy (Figure 2e,f).

2.2. JGCs Promoted Breast Cancer Cell Apoptosis. To reveal the underlying mechanisms responsible for the JGC-mediated inhibitory effects, apoptosis was detected by flow cytometry with Annexin V-fluorescein isothiocyanate (FITC)/propidium iodide (PI) double staining. JGCs concentration-dependently enhanced the apoptosis rate of TNBC cells. The apoptosis rate of MDA-MB-231 cells increased from 2.47 ± 0.21% (0.5 mg/mL) to 4.57 ± 0.42% (1 mg/mL) and 30.9 ± 1.09% (2 mg/mL) after 24 h of treatment with JGCs (Figure 3a,b). For MDA-MB-468 cells, the apoptosis percentage increased from 12.25 ± 0.32% (0.25 mg/ml) to 15.65 ± 0.74% (0.5 mg/mL) and 22.56 ± 0.79% (1 mg/mL) (Figure 3c,d). After 48 h, a similar apoptosis rate trend was observed

https://doi.org/10.1021/acsomega.2c01921
ACS Omega 2022, 7, 28003−28015

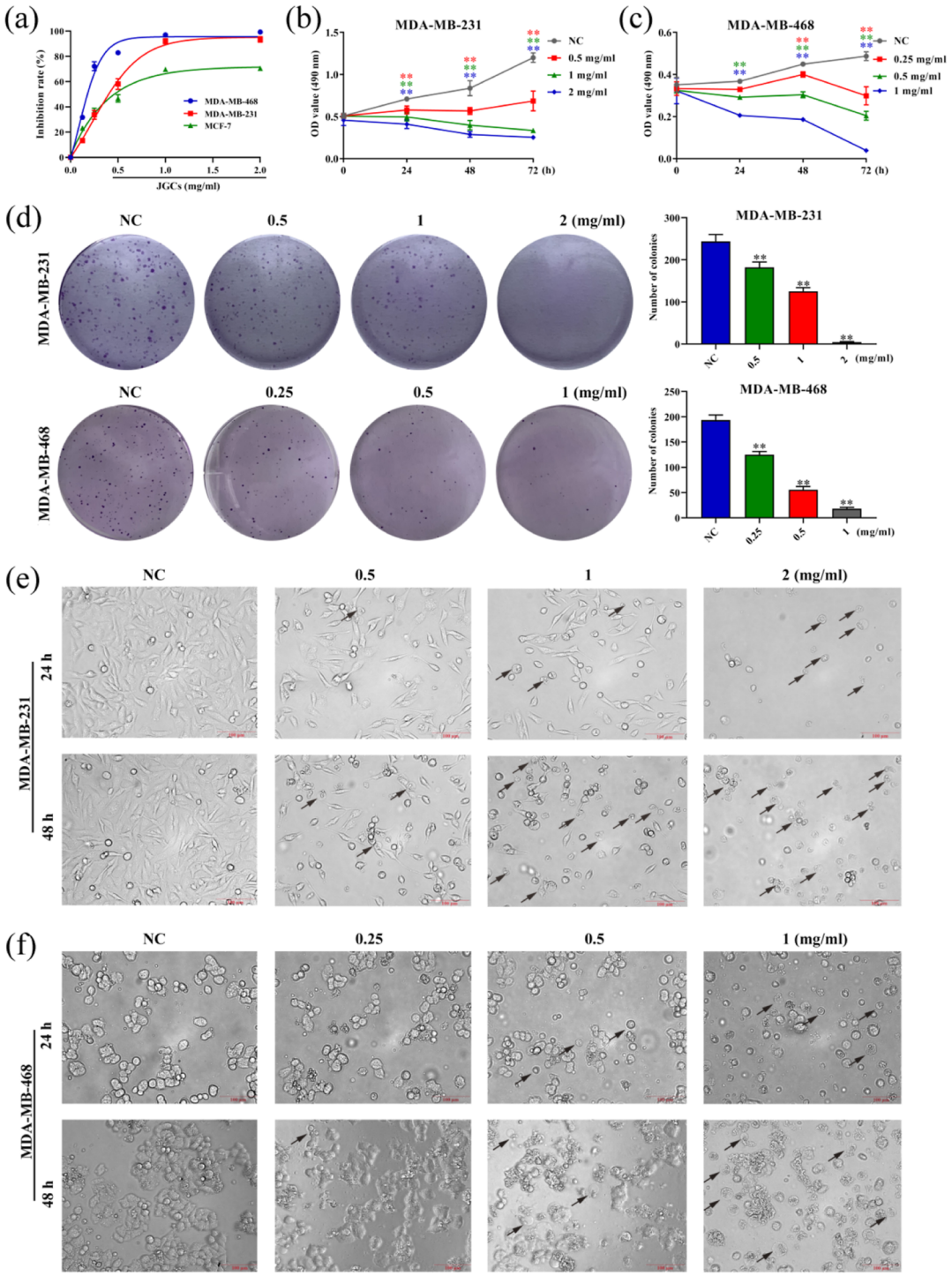

Figure 2. JGCs inhibited the viability and proliferation of breast cancer cells. (a) Cell viability was assessed by an MTT assay after JGC treatment for 72 h. (b,c) Cell proliferation of MDA-MB-231 (b) and MDA-MB-468 (c) cells treated with the indicated dose of JGCs was determined using the MTT assay. (d) Colony formation of MDA-MB-231 and MDA-MB-468 cells treated with JGCs. (e,f) Representative images of MDA-MB-231 (e) and MDA-MB-468 (f) cells treated with JGCs for 24 and 48 h (magnification ×200, scale bar: 100 μm) (black arrows indicate apoptotic cells). Each experiment was repeated at least in triplicate. $^{**}P < 0.01$ vs the control group.

after the cells were treated with JGCs. Moreover, at the same concentration, the apoptosis rate at 48 h was higher than that at 24 h. The morphological changes during cell apoptosis were then validated by Hoechst 33342 staining. As shown in Figure 3e,f, many MDA-MB-231 and MDA-MB-468 cell nuclei became noticeably dense and fragmented. These results suggest that JGCs are able to induce cell apoptosis in a concentration- and time-dependent manner.

2.3. JGCs Induced S Phase Cell Cycle Arrest in Breast Cancer Cells. We also evaluated the influence of JGCs on the cell cycle distribution using PI staining and flow cytometry. Compared with the control group, in MDA-MB-231 cells, JGC treatment at 0.5 and 1 mg/mL for 24 h led to the clear

https://doi.org/10.1021/acsomega.2c01921
ACS Omega 2022, 7, 28003−28015

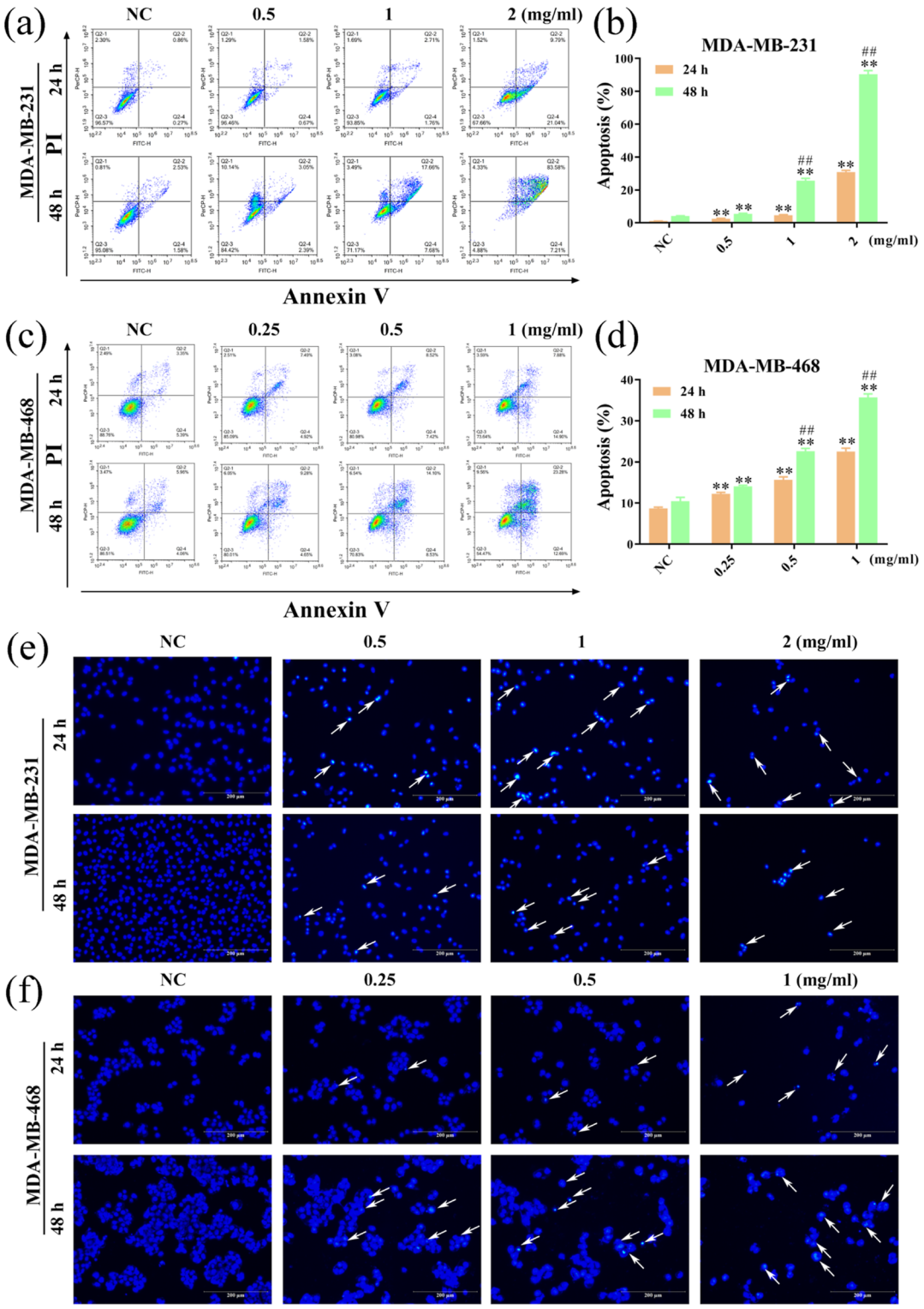

Figure 3. JGCs promoted breast cancer cell apoptosis. (a) Apoptosis analysis of MDA-MB-231 cells treated with different concentrations of JGCs for 24 or 48 h. (b) Histogram analysis of the percentage of total apoptotic MDA-MB-231 cells. (c) Apoptosis analysis of MDA-MB-468 cells treated with different concentrations of JGCs for 24 or 48 h. (d) Histogram analysis of the percentage of total apoptotic MDA-MB-468 cells. (e,f) MDA-MB-231 (e) and MDA-MB-468 (f) cells were stained with Hoechst 33258 and examined by fluorescence microscopy (magnification ×200, scale bar: 200 μm) (white arrows showing the bright blue regions indicate fragmented or condensed nuclei). Data are shown as the mean ± SD for treatments tested at least in triplicate. $^{**}P < 0.01$ vs the control group, $^{\#\#}P < 0.01$ vs the JGC 24 h group.

accumulation of cells in the S phase and a significant decrease in cells in G1 and G2 phases (Figure 4a,b). After 48 h of treatment, flow cytometry analysis showed that JGC treatment at 0.25, 0.5, and 1 mg/mL could significantly increase the percentage of MDA-MB-231 cells in the S phase. Consistent with the results in MDA-MB-231 cells, we observed that JGC treatment enhanced the proportion of MDA-MB-468 cells in the S phase and reduced the proportions of cells in G1 and G2

https://doi.org/10.1021/acsomega.2c01921
ACS Omega 2022, 7, 28003−28015

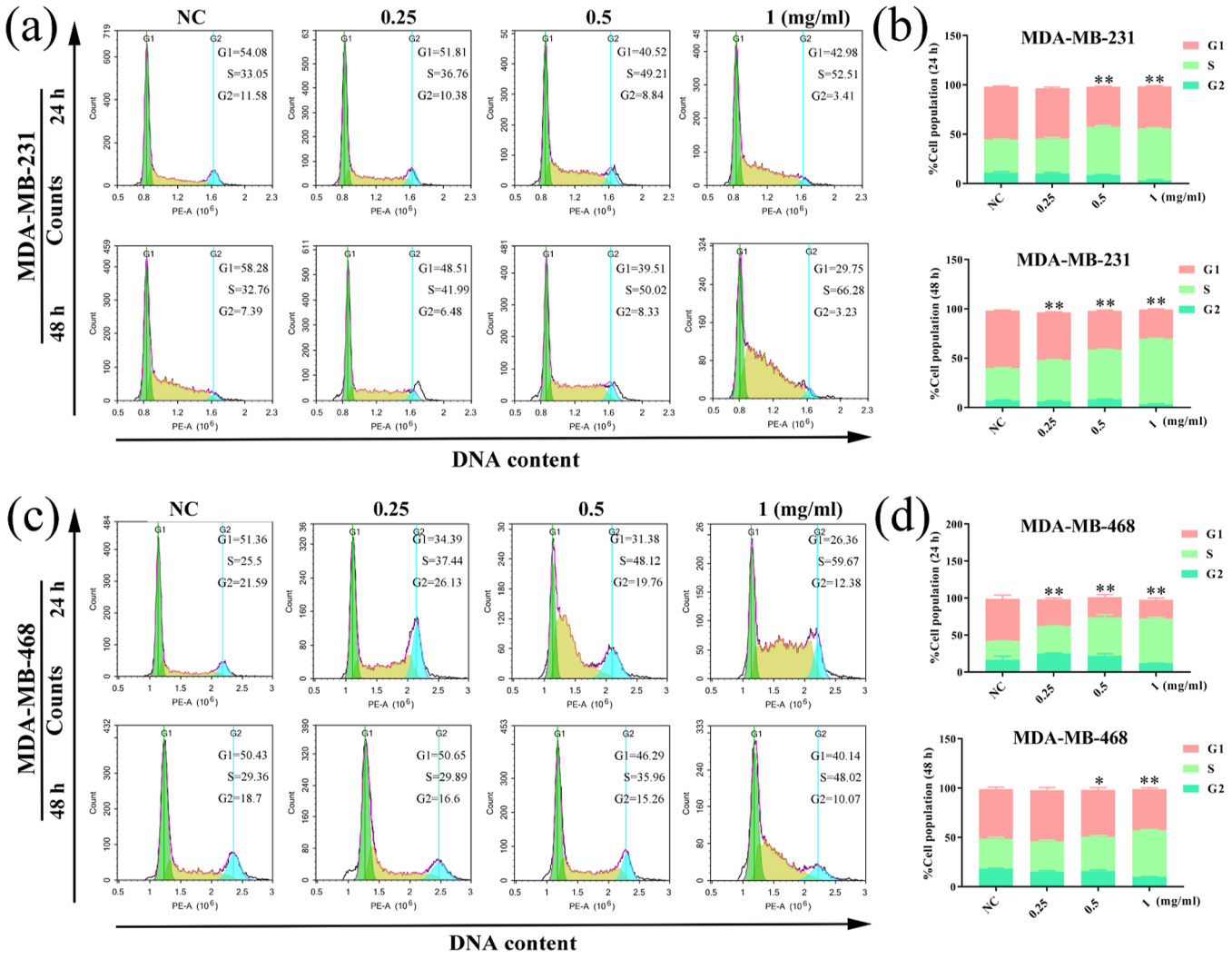

Figure 4. JGCs induced S phase cell cycle arrest in breast cancer cells. (a) The cell cycle distribution of MDA-MB-231 cells treated with JGCs was analyzed by flow cytometry. (b) Cell cycle distribution of MDA-MB-231 cells in the G1, S, and G2 phases. (c) The cell cycle distribution of MDA-MB-468 cells treated with JGCs was analyzed by flow cytometry. (d) Cell cycle distribution of MDA-MB-468 cells in the G1, S, and G2 phases. Each experiment was repeated at least in triplicate. $*P < 0.05$, $**P < 0.01$ vs the control group.

phases (Figure 4c,d). These findings indicate that the JGC-induced inhibitory effect on breast cancer cell proliferation is partly associated with arresting cell cycle progression at the S phase.

2.4. JGCs Regulated the Expression of Apoptosis- and Cell Cycle-Related Proteins in Breast Cancer Cells. To further explore the possible mechanisms of JGCs in breast cancer, Western blot analysis was performed to evaluate changes in the expression levels of apoptosis- and cell cycle-associated proteins. As shown in Figure 5a, JGCs promoted the concentration-dependent specific cleavage of poly(ADP-ribose) polymerase (PARP), caspase-8, caspase-9, and caspase-3 in both MDA-MB-231 and MDA-MB-468 cells. Moreover, the protein ratio of Bax/Bcl-2 also increased after 24 h of JGC treatment. These results together demonstrated that JGCs induced apoptosis in MDA-MB-231 and MDA-MB-468 cells probably via both the mitochondrial-dependent and extrinsic pathways. In addition, JGC treatment notably downregulated the levels of *c*-Myc, CDK2, cyclin B1, CDC25C, and *p*-CDC25C but upregulated the level of p21 (Figure 5b). These results further clarify that JGCs could arrest breast cancer cell cycle progression.

2.5. Identification of the Active Ingredients in JGCs. To determine the pharmacodynamic material basis of JGCs, UPLC-HR-MS/MS analysis was first carried out on an Agilent 1100 instrument and Thermo Ultimate 3000/Q EXACTIVE FOCUS mass spectrometers. As shown in Figure 6a, 45 ingredients were identified from JGCs. Detailed information on these ingredients is provided in Table S1. Further analysis revealed that these chemical constituents included 10 terpenoids, 10 phenylpropanoids, 8 ketones, 3 alcohols/ethers, 3 acids/esters, 2 phenols, 2 alkaloids, and 7 other compounds (Figure 6b). According to the OB and DL values, seven ingredients were identified as potential active ingredients, which might be responsible for the antitumor activities of JGCs (Table S2).

2.6. Identification of the Potential JGC Targets. Then, we investigated the possible genetic foundation of JGCs, and 234 targets of the 7 active ingredients in JGCs were retrieved from STITCH, TCMSP, ETCM, SymMap, and DrugBank. Furthermore, a total of 1460 genes were identified as breast cancer-related targets from CTD, TDD, DISEASES, and MalaCards. Venn diagram analysis showed that there were 116 JGC-related targets for breast cancer (Figure 7a). Then,

https://doi.org/10.1021/acsomega.2c01921
ACS Omega 2022, 7, 28003−28015

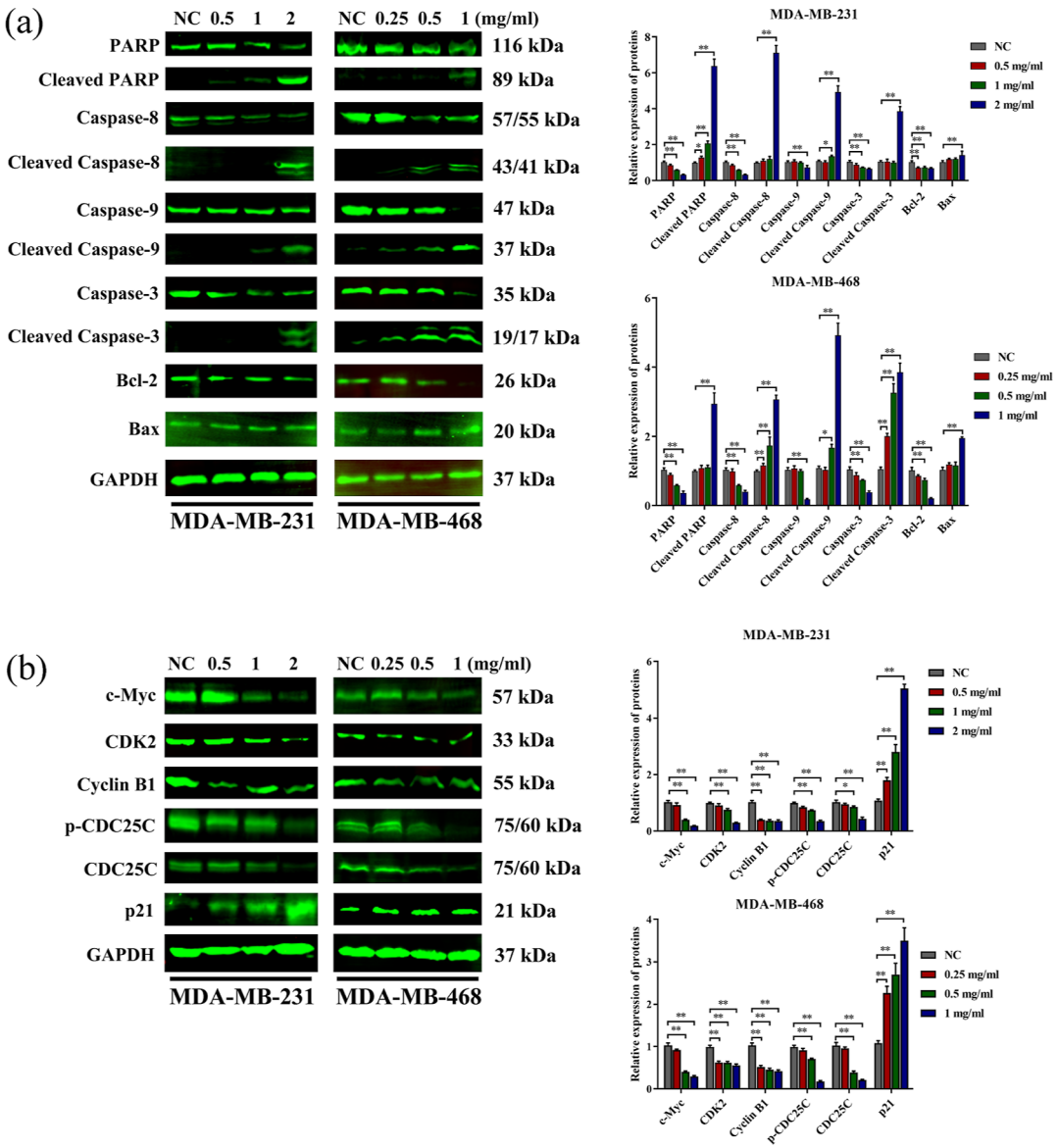

Figure 5. JGCs regulated the expression of apoptosis- and cell cycle-related proteins in breast cancer cells. (a) Western blot analysis of the effects of JGCs on apoptosis-related proteins, including Bcl-2, Bax, activated caspase-8, activated caspase-9, activated caspase-3, and PARP, in breast cancer cells after 24 h of treatment with JGCs. (b) Western blot analysis of the effects of JGCs on cell cycle-related proteins, including c-Myc, CDK2, cyclin B1, CDC25C, *p*-CDC25C, and p21, in JGC-treated cells. GAPDH was used as a loading control. Each experiment was repeated at least in triplicate.

we generated a protein−protein interaction (PPI) network for the 116 genes. From the network, we identified 10 hub genes, including JUN, RELA, MAPK14, STAT3, FOS, ESR1, NR3C1, EP300, MAPK1, and SRC, which might be the key targets of JGCs for the inhibition of breast cancer (Figure 7b). We also constructed an active ingredient−target interaction network for JGCs and found that puerarin, daidzein, dehydroandrographolide, neoandrographolide, eleutheroside B, cryptochlorogenic acid, and harpagoside had 51, 44, 11, 8, 7, 1, and 1 target genes, respectively (Figure 7c). Among the 116 genes, PTGS2 could potentially interact with all 7 active ingredients.

2.7. JGCs Inhibited Breast Cancer Tumorigenesis through the JAK2/STAT3 Signaling Pathway. To further elucidate the underlying mechanism by which JGCs exert their antibreast cancer activity, we performed the biological process and Kyoto encyclopedia of genes and genomes (KEGG) pathway enrichment analyses for the 116 JGC-related genes via Metascape. Gene ontology (GO) enrichment analysis revealed that these genes were prominently related to several biological processes, including cellular response to organic cyclic compounds ($P = 2.50 \times 10^{-39}$), positive regulation of cell death ($P = 2.50 \times 10^{-39}$), and the apoptotic signaling pathway ($P = 5.78 \times 10^{-34}$) (Figure 8a). Additionally, as shown in Figure 8b, there were many pathways potentially participating in the antitumor effects of JGCs, such as pathways in cancer ($P = 1.03 \times 10^{-49}$), apoptosis ($P = 4.81 \times 10^{-27}$), microRNAs in cancer ($P = 8.58 \times 10^{-25}$), and the Janus kinase (JAK)-signal transducer and activator of transcription (STAT) signaling pathway ($P = 4.55 \times 10^{-20}$).

Our previous studies reported that the JAK-STAT signaling pathway played major roles in the carcinogenesis process.[18,19] Recent studies have demonstrated that the JAK-STAT signaling pathway is also involved in the regulation of breast

https://doi.org/10.1021/acsomega.2c01921
ACS Omega 2022, 7, 28003−28015

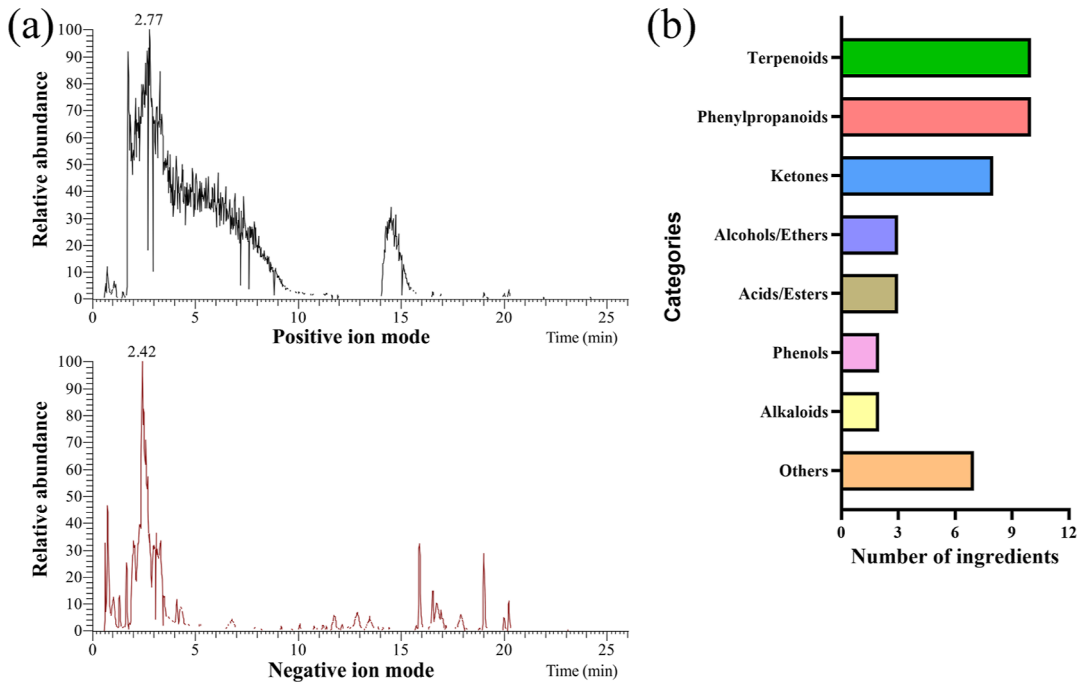

Figure 6. Identification of active ingredients in JGCs. (a) UPLC-HR-MS/MS analysis of JGCs in positive and negative ion modes. (b) Major categories of identified ingredients.

cancer cell proliferation, cycle arrest, and apoptosis.[20,21] Combined with the above KEGG analysis results, we attempted to determine whether the suppressive effect of JGCs on the breast cancer cell phenotype was mediated through the JAK-STAT signaling pathway. In both MDA-MB-231 and MDA-MB-468 cells, Western blot analysis showed that JGCs could markedly decrease the expression of *p*-JAK2, *p*-STAT3, and STAT3 in a dose-dependent manner but had no effect on the expression of total JAK2 (Figure 8c,d). Taken together, these results demonstrated that JGCs might exhibit their antibreast cancer effect by inactivating the JAK2/STAT3 signaling pathway.

3. DISCUSSION

TCMs have been applied for the prevention and treatment of breast cancer for thousands of years in China. In the present study, we evaluated the effects of JGCs on breast cancer cells. Our results demonstrated that JGCs significantly inhibited breast cancer cell growth in a dose- and time-dependent manner, promoted cell apoptosis, and induced cell cycle arrest in the S phase, indicating that JGCs may serve as a potential therapeutic drug against breast cancer; however, the identities of the effective substances remain unclear.

Generally, TCM exhibits multicomponent, multitarget, and multipathway biological effects. Considering the complexity, it is difficult to clarify how TCM actions are carried out by traditional methods. Based on systems biology, pharmacology, and bioinformatics approaches, network pharmacology has been validated as a powerful tool to uncover the molecular mechanisms of TCM and brings new opportunities to drug development.[22,23] For instance, network pharmacology combined with experimental evaluation was used to reveal the synergistic effects of Huachansu capsules on hepatocellular carcinoma cell proliferation and migration.[24] Despite its wide application in various human diseases, there are some limitations of network pharmacology to identify active ingredients. For example, shikimic acid was reported to be an active ingredient and promote ER-positive breast cancer cell proliferation.[25] However, it was excluded according to the OB and DL values in this study. Therefore, network pharmacology, as a bioinformatics approach, can provide some preliminary evidence but still requires experimental validation.

Utilizing UPLC-HR-MS/MS analysis and network pharmacology, we identified seven potential bioactive ingredients from JGCs. Interestingly, all seven ingredients have been identified as potential anti-inflammatory agents in various diseases, including osteoarthritis, ischemia−reperfusion injury, and colitis.[26−32] Moreover, some compounds have also shown potential antitumor activity. For example, puerarin, a natural isoflavonoid from *Pueraria lobata*, could restrain breast cancer cell metastasis and enhance chemosensitivity to adriamycin.[33,34] Daidzein, a natural isoflavone from Leguminosae, was found to induce cell cycle arrest at the G1 and G2/M phases, promote cell apoptosis, suppress TNF-α-induced migration and invasion, and reverse breast cancer resistance protein (BCRP)-mediated drug resistance in breast cancer.[35−38] Eleutheroside B (syringin), a phenylpropanoid glycoside, can induce oxidative stress to suppress the proliferation of breast cancer.[39] Neoandrographolide and dehydroandrographolide, the two principal components of *A. paniculata* (Burm.f.) Nees, had shown good antitumor effects against a variety of tumor cells, including Jurkat cells, lung cancer cells, and oral cancer cells. However, their biological functions in breast cancer remain unclear.[40−42] The bioactivities of other bioactive ingredients, including harpagoside and cryptochlorogenic acid, against human cancer have not yet been reported.

Applying Venn analysis, 116 target genes of the 7 bioactive ingredients were identified as potential targets of JGCs responsible for their inhibitory effects against breast cancer. In the bioactive compound−target interaction network, we observed that PTGS2 was the common target of the seven bioactive ingredients. PTGS2 encodes the inducible enzyme

https://doi.org/10.1021/acsomega.2c01921
ACS Omega 2022, 7, 28003−28015

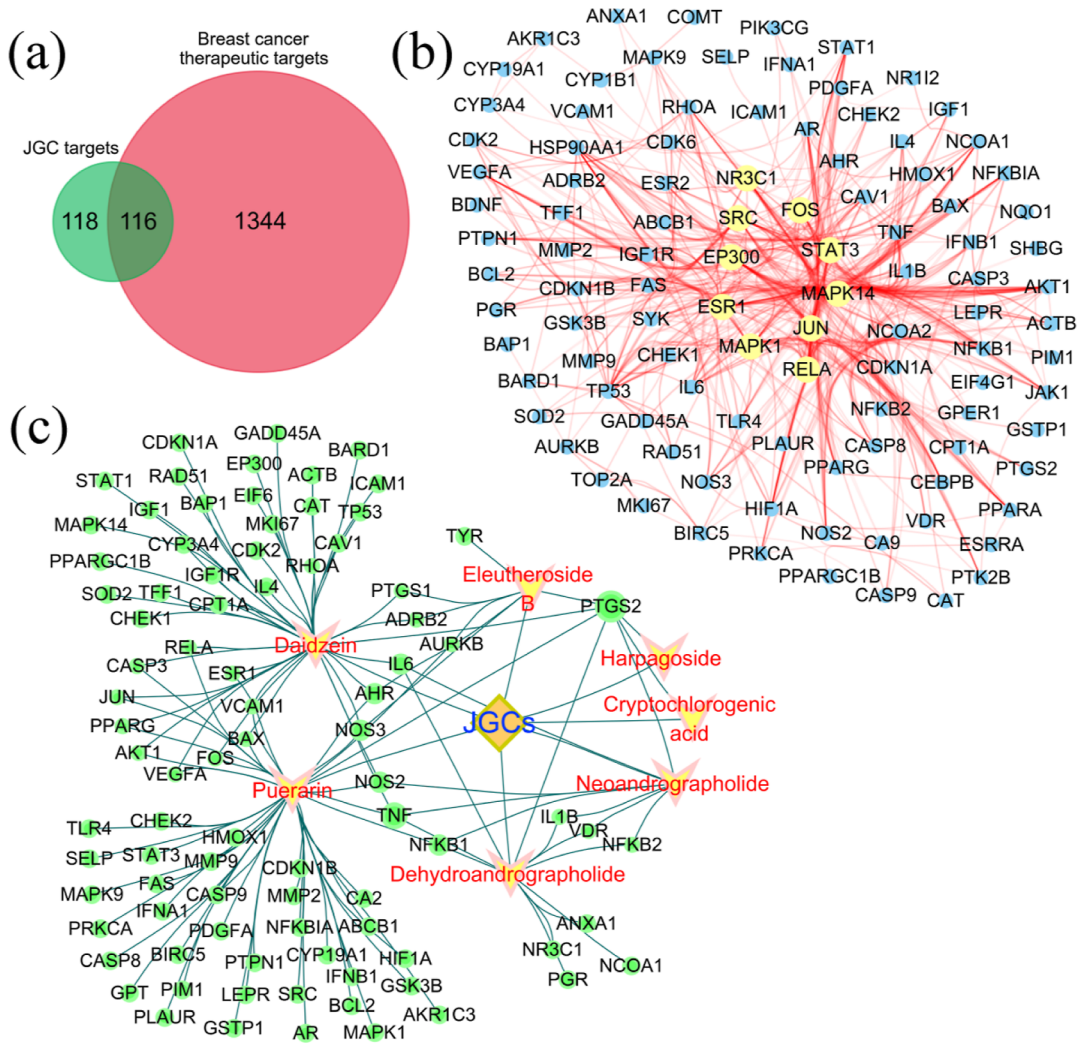

Figure 7. Identification of the potential JGC targets. (a) Venn diagram analysis of the overlapping targets. We filtered out 116 potential JGC targets in breast cancer. (b) PPI network of 116 JGC-related targets in breast cancer using STRING. The interaction score was set as the highest confidence (0.900). (c) An active ingredient−target network was generated using Cytoscape, which consisted of 7 active ingredients and 116 potential targets. The red triangles represent the active ingredients. The green circles represent the gene that the ingredient targets.

COX-2, which converts arachidonic acid into prostaglandins. PTGS2 is frequently highly expressed in several types of human cancer, including breast cancer, and predicts an unfavorable prognosis.[43] PTGS2 was reported to promote breast cancer cell invasion and enhance chemoresistance and stemness.[44−46] Other target genes, such as NFKB1, NOS2, and AURKB, also have crucial roles in breast cancer tumorigenesis.[47−49]

Subsequently, gene function enrichment analysis of the 116 target genes was performed to comprehensively understand the possible mechanisms. The results showed marked enrichment in the positive regulation of cell death and the apoptotic signaling pathway, which was in accordance with our observation of JGCs promoting breast cancer cell apoptosis. Consistent with their known anti-inflammatory roles, we found that these genes were strongly associated with the response to lipopolysaccharide, indicating that JGCs might have the potential to modulate breast cancer immunotherapy. Interestingly, the positive regulation of cell migration was also implicated for JGCs.

KEGG pathway analysis revealed that the antitumor effects of JGCs might be involved in apoptosis, cancer, and the JAK-STAT signaling pathway. Notably, the JAK-STAT signaling pathway has also been implicated in tumor survival, metastasis, angiogenesis, apoptosis, and drug resistance, suggesting that the JAK-STAT pathway is a promising therapeutic target for breast cancer treatment.[50] Several reports have shown that TCMs can arrest tumorigenesis and metastasis by regulating the JAK-STAT signaling pathway. For example, ECN, a compound derived from *Tussilago farfara* L. (Kuan Dong Hua), downregulated the expression of phosphorylated JAK1/2 and Src, blocked the nuclear translocation of STAT3, and induced apoptosis of breast cancer cells.[51] Yang et al. identified a STAT3 inhibitor from *Eupatorium lindleyanum* that strongly inhibited the viability of TNBC cells.[52] In accordance with the KEGG analysis, the Western blot results showed that the protein expression of *p*-JAK2, *p*-STAT3, and STAT3 was significantly decreased after JGC treatment. These findings highlighted that JGCs might exert their antibreast cancer effects partly by inhibiting the JAK/STAT signaling pathway.

4. CONCLUSIONS

In conclusion, our study provides the first clear evidence of JGCs having excellent antitumor activity against breast cancer.

https://doi.org/10.1021/acsomega.2c01921
ACS Omega 2022, 7, 28003−28015

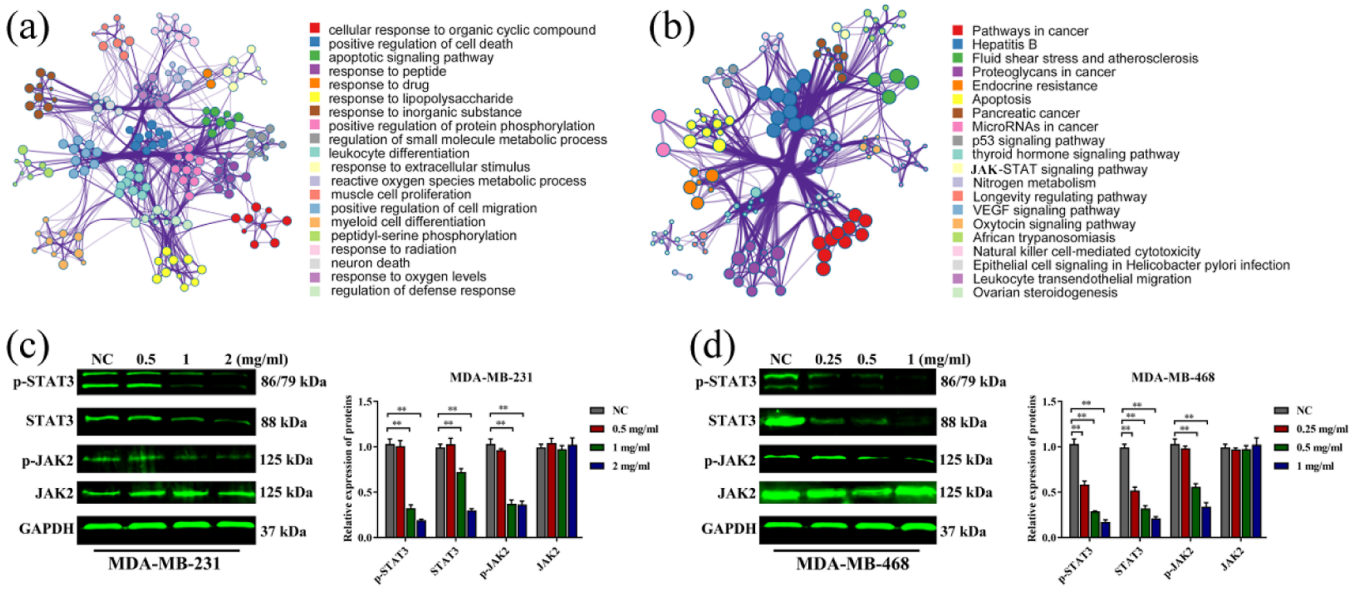

Figure 8. JGCs inhibited breast cancer tumorigenesis through the JAK2/STAT3 signaling pathway. (a) The top 20 biological processes were enriched using Metascape. (b) The top 20 KEGG pathways were identified using Metascape. (c,d) Western blot analysis of *p*-JAK2, JAK2, *p*-STAT3, and STAT3 in breast cancer cells after 24 h of treatment with JGCs. GAPDH was used as a loading control. Each experiment was repeated at least in triplicate.

Furthermore, JGCs significantly repressed cell growth, promoted cell apoptosis, and induced S phase cell cycle arrest partly by inactivating the JAK2/STAT3 signaling pathway. Additionally, we identified many potential active ingredients from JGCs that may help develop novel therapeutic agents against breast cancer.

5. MATERIALS AND METHODS

5.1. Preparation of JGCs. JGCs were purchased from Guizhou Bailing Enterprise Group Pharmaceutical Corporation Limited (Guiyang, China). JGCs were prepared according to a previous patent (CN201010137089.8) by Guizhou Bailing. Briefly, the raw materials consisted of the flowers of *L. japonica* Thunb. (250 g), the dried aerial part of *Andrographis paniculate* (Burm.f.) Nees (250 g), the root of *I. tinctoria* L. (250 g), the dried whole plant of *T. mongolicum* Hand.-Mazz. (250 g), acetaminophen (250 g), amantadine hydrochloride (50 g), and chlorphenamine maleate (1.0 g). The alcohol extracts of *A. paniculata* (Burm.f.) Nees were obtained using 10 volumes of 85% ethanol for 2 h and 8 volumes for 2 h of 85% ethanol, *I. tinctoria* L., and *T. mongolicum* Hand.-Mazz. Also, the drug residues of *L. japonica* Thunb. were decocted with water twice with 7 and 5 solvent volumes for 1.5 h each time. The above alcohol extracts and aqueous extracts were mixed with acetaminophen, amantadine hydrochloride, and chlorphenamine maleate; dried; crushed into 20 mesh particles; dried again; and mixed with the distillate of *L. japonica* Thunb. The total mixture was filled into capsules and packed. A total of 1000 capsules were generated.

5.2. Cell Culture and Treatment. The human breast cancer cell lines MCF-7, MDA-MB-231, and MDA-MB-468 were purchased from the American Type Culture Collection (ATCC, Manassas, VA, USA). All cells were maintained in Dulbecco's modified Eagle's medium (DMEM; GIBCO, USA) at 37 °C with 5% CO_2 supplemented with 10% fetal bovine serum (FBS; GIBCO, USA). According to a previous description,[24] pulverized JGCs (0.45 g) were accurately weighed and dissolved in 2.25 mL of phosphate-buffered saline (PBS), processed with ultrasonication for 30 min, centrifuged at 3000 rpm for 15 min, filtered through a 0.22 μm nylon membrane (Millipore, USA) at a final concentration of 0.2 g/mL, and diluted with the culture medium to different concentrations (0.125, 0.25, 0.5, 1, or 2 mg/mL).

5.3. MTT Assay. A total of 6000 cells were seeded to 96-well plates. After culturing overnight, the cells were treated with PBS or various concentrations of JGCs (0, 0.125, 0.25, 0.5, 1, or 2 mg/mL) for the indicated time. Then, 10 μL of 3-(4,5-dimethylthiazol-2-yl)-2,5-diphenyl-2H-tetrazolium bromide (MTT) solution (Sigma, USA) was added to each well and incubated for 4 h at 37 °C. Afterward, the supernatant was removed, and 160 μL of dimethyl sulfoxide (DMSO) was added to each well. The absorbance value at 490 nm was measured using a microplate reader (BioTek, Winooski, VT, USA). The IC_{50} values were estimated by the relative survival curve.

5.4. Colony Formation Assay. Cells were seeded in 6-well plates (1000 cells/well). After treatment with the indicated concentration of JGCs for 14 days, the colonies were fixed with 4% paraformaldehyde (PFA; Sigma) for 30 min and stained with a 0.1% crystal violet solution (Sigma) for 20 min. Images were captured with a digital camera, and the visible colonies were counted.

5.5. Flow Cytometry Analysis. Cells were seeded into 6-well plates and exposed to JGCs for 24 and 48 h. For the cell apoptosis assay, the cells were stained using an FITC Annexin V/PI apoptosis detection kit (BD Biosciences, Franklin Lakes, NJ, USA) in the dark for 15 min at room temperature and analyzed using a FACSCalibur flow cytometer (BD Biosciences). For the cell cycle assay, cells were fixed with 70% ethanol at −20 °C overnight, stained with PI (BD Biosciences) in the dark for 30 min at 37 °C, and then measured by flow cytometry.

5.6. Hoechst 33258 Staining. Hoechst 33258 staining was performed to observe the nuclear morphology of the

https://doi.org/10.1021/acsomega.2c01921
ACS Omega 2022, 7, 28003−28015

apoptotic cells according to a previous description.[53] Briefly, after treatment with different concentrations of JGCs, cells were stained with Hoechst 33258 (Beyotime, Jiangsu, China) for 10 min. The stained nuclei were observed under a Leica fluorescence microscope.

5.7. Western Blot. Treated cells were harvested and lysed in radioimmunoprecipitation assay (RIPA) buffer with a protease inhibitor cocktail. Proteins were separated by 8−12% sodium dodecyl sulfate polyacrylamide gel electrophoresis (SDS-PAGE) and transferred to polyvinylidene difluoride (PVDF) membranes. The membranes were blocked with 5% nonfat milk for 1 h at room temperature and then incubated with primary antibodies against caspase-3, cleaved caspase-3, caspase-8, cleaved caspase-8, caspase-9, cleaved caspase-9, PARP, Bcl-2, Bax, CDK2, cyclin B1, *c*-Myc, CDC25C, *p*-CDC25C, p21, JAK2, *p*-JAK2, STAT3, *p*-STAT3, and GAPDH (CST, Danvers, MA, USA) at 4 °C. After overnight incubation, the membranes were incubated with fluorescently labeled secondary antibodies (CST) for 1 h at room temperature. The protein levels were normalized to GAPDH.

5.8. UPLC-HR-MS/MS Analysis. Pulverized JGCs were accurately weighed and dissolved. The JGC ingredients were identified by UPLC-HR-MS/MS system analysis on an Agilent 1100 instrument and Thermo Ultimate 3000/Q EXACTIVE FOCUS mass spectrometers (Thermo Finnigan, San Jose, CA, USA). Chromatographic separation was performed on an ACE Ultracore 2.5 SuperC18 column (2.1 mm × 100 mm). The column temperature was 40 °C, the flow rate was 0.3 mL/min, mobile phase A was a 0.1% aqueous solution of formic acid, and mobile phase B was acetonitrile. The data were analyzed in both positive and negative ion modes with a UHPLC-Q/Exactive instrument with the following parameters: electrospray ionization (ESI) source; spray voltage: 3.0 kV (+)/2.5 kV (−); scanning model: full MS-ddms2; resolution: full MS (70,000) and MS/MS (17,500); isolation width: 1.5 *m*/*z*; intensity threshold: 1.6×10^5; and dynamic execution: 5 s. The temperature of the capillary tube was 320 °C, followed by heating to 350 °C. The flow rates of the sheath and auxiliary gas were 35.0 and 10.0 arbitrary units, respectively. Then, the collected raw data were imported into Compound Discoverer 3.0 software to perform qualitative analysis. The measured spectra of the secondary fragments were matched with the mzCloud network database and the Orbitrap Traditional Chinese Medicine Library (OTCML).[54] The UPLC-HR-MS/MS analysis was conducted at the Analysis and Testing Center of The Key Laboratory of Chemistry for Natural Products of Guizhou Province and Chinese Academic of Sciences.

5.9. Screening the Active Ingredients of the JGCs. All ingredients obtained from UPLC-HR-MS/MS were analyzed using TCMSP,[55] TCM Database@Taiwan,[56] ETCM,[57] and SymMap.[58] Ingredients with OB ≥ 10% and DL ≥ 0.10 were defined as potential active ingredients for further analysis.[59,60]

5.10. Target Fishing of JGCs and Breast Cancer. Targets of the potential active ingredients in the JGCs were retrieved from STITCH,[61] TCMSP,[55] ETCM,[57] SymMap,[58] and DrugBank.[62] Breast cancer-related targets were collected from CTD,[63] TDD,[64] DISEASES,[65] and MalaCards.[66]

5.11. Target Mapping and Network Construction. Venn diagram analysis was employed to search for target genes common for both the active ingredients and breast cancer. The JGC-active ingredient−target network was constructed using Cytoscape_3.6.0.[67] GO and KEGG pathway enrichment analyses were performed using Metascape.[68] Then, the enriched pathway terms with a *P* value less than 0.05 were considered significant and selected for further analysis. A PPI network was generated using STRING,[69] and hub genes from the network were identified using cytoHubba.[70]

5.12. Statistical Analysis. All data from at least three independent experiments were analyzed using GraphPad Prism software and are presented as the mean ± standard deviation. The differences between groups were determined by a Student's *t*-test. $P < 0.05$ was considered significant.

■ ASSOCIATED CONTENT

Supporting Information

The Supporting Information is available free of charge at https://pubs.acs.org/doi/10.1021/acsomega.2c01921.

Major ingredients identified in JGCs via UPLC-HR-MS/MS analysis and seven potential active ingredients of JGCs (PDF)

■ AUTHOR INFORMATION

Corresponding Authors

Hui Song − *The Key Laboratory of Chemistry for Natural Products of Guizhou Province and Chinese Academic of Sciences & Key Laboratory of Endemic and Ethnic Diseases, Ministry of Education & Key Laboratory of Medical Molecular Biology of Guizhou Province, Guizhou Medical University, Guiyang 550004, China*; Email: songhui620@126.com

Jue Yang − *State Key Laboratory of Functions and Applications of Medicinal Plants, Guizhou Medical University, Guiyang 550014, China; State Key Laboratory of Drug Research, Shanghai Institute of Materia Medica, Chinese Academy of Sciences, Shanghai 201203, China; The Key Laboratory of Chemistry for Natural Products of Guizhou Province and Chinese Academic of Sciences & Key Laboratory of Endemic and Ethnic Diseases, Ministry of Education & Key Laboratory of Medical Molecular Biology of Guizhou Province, Guizhou Medical University, Guiyang 550004, China*; orcid.org/0000-0002-6150-8890; Email: yaodadewo@163.com

Yanmei Li − *State Key Laboratory of Functions and Applications of Medicinal Plants, Guizhou Medical University, Guiyang 550014, China; State Key Laboratory of Drug Research, Shanghai Institute of Materia Medica, Chinese Academy of Sciences, Shanghai 201203, China; The Key Laboratory of Chemistry for Natural Products of Guizhou Province and Chinese Academic of Sciences & Key Laboratory of Endemic and Ethnic Diseases, Ministry of Education & Key Laboratory of Medical Molecular Biology of Guizhou Province, Guizhou Medical University, Guiyang 550004, China*; Email: liyanmei518@hotmail.com

Authors

Jianfei Qiu − *State Key Laboratory of Functions and Applications of Medicinal Plants, Guizhou Medical University, Guiyang 550014, China; State Key Laboratory of Drug Research, Shanghai Institute of Materia Medica, Chinese Academy of Sciences, Shanghai 201203, China; The Key Laboratory of Chemistry for Natural Products of Guizhou Province and Chinese Academic of Sciences & Key Laboratory of Endemic and Ethnic Diseases, Ministry of Education & Key Laboratory of Medical Molecular Biology*

https://doi.org/10.1021/acsomega.2c01921
ACS Omega 2022, 7, 28003−28015

of Guizhou Province, Guizhou Medical University, Guiyang 550004, China

Zhiyin Zhang − *Guiyang Hospital of Guizhou Aviation Industry Group, Guiyang 550025, China*

Anling Hu − *State Key Laboratory of Functions and Applications of Medicinal Plants, Guizhou Medical University, Guiyang 550014, China; State Key Laboratory of Drug Research, Shanghai Institute of Materia Medica, Chinese Academy of Sciences, Shanghai 201203, China; The Key Laboratory of Chemistry for Natural Products of Guizhou Province and Chinese Academic of Sciences & Key Laboratory of Endemic and Ethnic Diseases, Ministry of Education & Key Laboratory of Medical Molecular Biology of Guizhou Province, Guizhou Medical University, Guiyang 550004, China*

Peng Zhao − *State Key Laboratory of Functions and Applications of Medicinal Plants, Guizhou Medical University, Guiyang 550014, China; State Key Laboratory of Drug Research, Shanghai Institute of Materia Medica, Chinese Academy of Sciences, Shanghai 201203, China; The Key Laboratory of Chemistry for Natural Products of Guizhou Province and Chinese Academic of Sciences & Key Laboratory of Endemic and Ethnic Diseases, Ministry of Education & Key Laboratory of Medical Molecular Biology of Guizhou Province, Guizhou Medical University, Guiyang 550004, China*

Xuenai Wei − *State Key Laboratory of Functions and Applications of Medicinal Plants, Guizhou Medical University, Guiyang 550014, China; State Key Laboratory of Drug Research, Shanghai Institute of Materia Medica, Chinese Academy of Sciences, Shanghai 201203, China; The Key Laboratory of Chemistry for Natural Products of Guizhou Province and Chinese Academic of Sciences & Key Laboratory of Endemic and Ethnic Diseases, Ministry of Education & Key Laboratory of Medical Molecular Biology of Guizhou Province, Guizhou Medical University, Guiyang 550004, China*

Complete contact information is available at: https://pubs.acs.org/10.1021/acsomega.2c01921

Author Contributions

Y.L. and J.Y. designed and conceived the study. J.Y., H.S., and J.Q. drafted the manuscript. J.Q., Z.Z., A.H., P.Z., and X.W. participated in experiments. Y.L., J.Y., and H.S. revised the manuscript. All authors contributed to the article and approved the submitted version.

Notes

The authors declare no competing financial interest.

■ ACKNOWLEDGMENTS

This study was supported by grants from the National Natural Science Foundation of China (82160813, 32060210, 81872772, 81960546, and U1812403), the State Key Laboratory of Drug Research (SIMM2105KF-15), the Science and Technology Department of Guizhou Province (QKHJC[2018]1409, QKHZC[2019]2762, QKHPTRC[2020]5008, and QKHZC[2020]4Y203), the 100 Leading Talents of Guizhou Province (fund for Y. M. L), P2018-KF11, QZYY-2019-022, the Guizhou Provincial Science and Technology Projects (QKHZK[2021]526 and QKHZK[2021]448), the Project of Key Laboratory of Endemic and Ethnic Diseases, Ministry of Education, Guizhou Medical University (QJHKY[2020]251), the Cultivation Project of the National Natural Science Foundation of China of Guizhou Medical University (20NSP064 and 19NSP008), (Qian Ke He Ping Tai Ren Cai (2019])5106, TianchanziJzi (2021)07, and GHGYYY-KYLX-2022-18.

■ ABBREVIATIONS

DMEM, Dulbecco's modified Eagle's medium
DMSO, dimethyl sulfoxide
FBS, fetal bovine serum
GO, gene ontology
JGCs, Jin'gan capsules
KEGG, Kyoto encyclopedia of genes and genomes
MTT, 3-(4,5-dimethylthiazol-2-yl)-2,5-diphenyltetrazolium-bromide
PPI, protein−protein interaction
PBS, phosphate-buffered saline
PFA, paraformaldehyde
PI, propidium iodide
SDS-PAGE, sodium dodecyl sulfate polyacrylamide gel electrophoresis
TCM, traditional Chinese medicine
UPLC-HR-MS/MS, ultra-performance liquid chromatography−high-resolution tandem mass spectrometry

■ REFERENCES

(1) Sung, H.; Ferlay, J.; Siegel, R. L.; Laversanne, M.; Soerjomataram, I.; Jemal, A.; Bray, F. Global Cancer Statistics 2020: GLOBOCAN Estimates of Incidence and Mortality Worldwide for 36 Cancers in 185 Countries. Global Cancer Statistics 2020: GLOBOCAN Estimates of Incidence and Mortality Worldwide for 36 Cancers in 185 Countries. *Ca-Cancer J. Clin.* **2021**, *71*, 209−249.

(2) Trayes, K. P.; Cokenakes, S. Breast Cancer Treatment. *Am. Fam. Physician* **2021**, *104*, 171−178.

(3) Wimmer, K.; Bolliger, M.; Bago-Horvath, Z.; Steger, G.; Kauer-Dorner, D.; Helfgott, R.; Gruber, C.; Moinfar, F.; Mittlböck, M.; Fitzal, F. Impact of Surgical Margins in Breast Cancer After Preoperative Systemic Chemotherapy on Local Recurrence and Survival. *Ann. Surg. Oncol.* **2020**, *27*, 1700−1707.

(4) Kumar, P.; Aggarwal, R. An overview of triple-negative breast cancer. *Arch. Gynecol. Obstet.* **2016**, *293*, 247−269.

(5) Wu, Y.; Cheng, C. S.; Li, Q.; Chen, J. X.; Lv, L. L.; Xu, J. Y.; Zhang, K. Y.; Zheng, L. The Application of Citrus folium in Breast Cancer and the Mechanism of Its Main Component Nobiletin: A Systematic Review. *J. Evidence-Based Complementary Altern. Med.* **2021**, *2021*, 2847466.

(6) Zhu, M.; Lyu, Z. Analysis on the clinical profiling of current prominent TCM doctors on treatment of breast cancer. *China J. Tradit. Chin. Med. Pharm.* **2019**, *34*, 3162−3166.

(7) Du, J.; Wang, L.; Huang, X.; Zhang, N.; Long, Z.; Yang, Y.; Zhong, F.; Zheng, B.; Lan, W.; Lin, W.; et al. Shuganning injection, a traditional Chinese patent medicine, induces ferroptosis and suppresses tumor growth in triple-negative breast cancer cells. *Phytomedicine* **2021**, *85*, 153551.

(8) Zhao, X.; Liu, J.; Feng, L.; Ge, S.; Yang, S.; Chen, C.; Li, X.; Peng, L.; Mu, Y.; Wang, Y.; et al. Anti-angiogenic effects of Qingdu granule on breast cancer through inhibiting NFAT signaling pathway. *J. Ethnopharmacol.* **2018**, *222*, 261−269.

(9) Zheng, W.; Han, S.; Jiang, S.; He, X.; Li, X.; Ding, H.; Cao, M.; Li, P. Antitumor effects of Xi Huang pills on MDA-MB-231 cells in vitro and in vivo. *Mol. Med. Rep.* **2018**, *18*, 2068−2078.

(10) Li, Y.; Li, X.; Cuiping, C.; Pu, R.; Weihua, Y. Study on the Anticancer Effect of an Astragaloside- and Chlorogenic Acid-Containing Herbal Medicine (RLT-03) in Breast Cancer. *J. Evidence-Based Complementary Altern. Med.* **2020**, *2020*, 1515081.

(11) Yu, J. K.; Yue, C. H.; Pan, Y. R.; Chiu, Y. W.; Liu, J. Y.; Lin, K. I.; Lee, C. J. Isochlorogenic Acid C Reverses Epithelial-Mesenchymal Transition via Down-regulation of EGFR Pathway in MDA-MB-231 cells. *Anticancer Res.* **2018**, *38*, 2127−2135.
(12) Rajaratinam, H.; Nafi, S.; Mohd Nafi, S. N. Andrographolide is an Alternative Treatment to Overcome Resistance in ER-Positive Breast Cancer via Cholesterol Biosynthesis Pathway. *Malays. J. Med. Sci.* **2019**, *26*, 6−20.
(13) Beesetti, S. L.; Jayadev, M.; Subhashini, G. V.; Mansour, L.; Alwasel, S.; Harrath, A. H. Andrographolide as a Therapeutic Agent Against Breast and Ovarian Cancers. *Open Life Sci.* **2019**, *14*, 462−469.
(14) Liu, Z.; Tang, Y.; Zhou, R.; Shi, X.; Zhang, H.; Liu, T.; Lian, Z.; Shi, X. Bi-directional solid fermentation products of Trametes robiniophila Murr with Radix Isatidis inhibit proliferation and metastasis of breast cancer cells. *J. Chin. Med. Assoc.* **2018**, *81*, 520−530.
(15) Li, X. H.; He, X. R.; Zhou, Y. Y.; Zhao, H. Y.; Zheng, W. X.; Jiang, S. T.; Zhou, Q.; Li, P. P.; Han, S. Y. Taraxacum mongolicum extract induced endoplasmic reticulum stress associated-apoptosis in triple-negative breast cancer cells. *J. Ethnopharmacol.* **2017**, *206*, 55−64.
(16) Deng, X. X.; Jiao, Y. N.; Hao, H. F.; Xue, D.; Bai, C. C.; Han, S. Y. Taraxacum mongolicum extract inhibited malignant phenotype of triple-negative breast cancer cells in tumor-associated macrophages microenvironment through suppressing IL-10 / STAT3 / PD-L1 signaling pathways. *J. Ethnopharmacol.* **2021**, *274*, 113978.
(17) Afshar, E.; Hashemi-Arabi, M.; Salami, S.; Peirouvi, T.; Pouriran, R. Screening of acetaminophen-induced alterations in epithelial-to-mesenchymal transition-related expression of microRNAs in a model of stem-like triple-negative breast cancer cells: The possible functional impacts. *Gene* **2019**, *702*, 46−55.
(18) Hu, M.; Varier, K. M.; Li, Z.; Qin, X.; Rao, Q.; Song, J.; Hu, A.; Hang, Y.; Yuan, C.; Gajendran, B.; et al. A natural acylphloroglucinol triggered antiproliferative possessions in HEL cells by impeding STAT3 signaling and attenuating angiogenesis in transgenic zebrafish model. *Biomed. Pharmacother.* **2021**, *141*, 111877.
(19) Li, Y.; Shi, Y.; McCaw, L.; Li, Y. J.; Zhu, F.; Gorczynski, R.; Duncan, G. S.; Yang, B.; Ben-David, Y.; Spaner, D. E. Micro-environmental interleukin-6 suppresses toll-like receptor signaling in human leukemia cells through miR-17/19A. *Blood* **2015**, *126*, 766−778.
(20) To, N. B.; Nguyen, Y. T.; Moon, J. Y.; Ediriweera, M. K.; Cho, S. K. Pentadecanoic Acid, an Odd-Chain Fatty Acid, Suppresses the Stemness of MCF-7/SC Human Breast Cancer Stem-Like Cells through JAK2/STAT3 Signaling. *Nutrients* **2020**, *12*, 1663.
(21) Chen, D.; Ma, Y.; Li, P.; Liu, M.; Fang, Y.; Zhang, J.; Zhang, B.; Hui, Y.; Yin, Y. Piperlongumine Induces Apoptosis and Synergizes with Doxorubicin by Inhibiting the JAK2-STAT3 Pathway in Triple-Negative Breast Cancer. *Molecules* **2019**, *24*, 2338.
(22) Ye, H.; Wei, J.; Tang, K.; Feuers, R.; Hong, H. Drug Repositioning Through Network Pharmacology. *Curr. Top. Med. Chem.* **2016**, *16*, 3646−3656.
(23) Yuan, H.; Ma, Q.; Cui, H.; Liu, G.; Zhao, X.; Li, W.; Piao, G. How Can Synergism of Traditional Medicines Benefit from Network Pharmacology? *Molecules* **2017**, *22*, 1135.
(24) Huang, J.; Chen, F.; Zhong, Z.; Tan, H. Y.; Wang, N.; Liu, Y.; Fang, X.; Yang, T.; Feng, Y. Interpreting the Pharmacological Mechanisms of Huachansu Capsules on Hepatocellular Carcinoma Through Combining Network Pharmacology and Experimental Evaluation. *Front. Pharmacol.* **2020**, *11*, 414.
(25) Ma, X.; Ning, S. Shikimic acid promotes estrogen receptor-(ER)-positive breast cancer cells proliferation via activation of NF-κB signaling. *Toxicol. Lett.* **2019**, *312*, 65−71.
(26) Haseeb, A.; Ansari, M. Y.; Haqqi, T. M. Harpagoside suppresses IL-6 expression in primary human osteoarthritis chondrocytes. *J. Orthop. Res.* **2017**, *35*, 311−320.
(27) Liu, Y.; Liu, Y.; Zhang, H. L.; Yu, F. F.; Yin, X. R.; Zhao, Y. F.; Ye, F.; Wu, X. Q. Amelioratory effect of neoandrographolie on myocardial ischemic-reperfusion injury by its anti-inflammatory and anti-apoptotic activities. *Environ. Toxicol.* **2021**, *36*, 2367−2379.
(28) Jeon, Y. D.; Lee, J. H.; Lee, Y. M.; Kim, D. K. Puerarin inhibits inflammation and oxidative stress in dextran sulfate sodium-induced colitis mice model. *Biomed. Pharmacother.* **2020**, *124*, 109847.
(29) Zhao, X. L.; Yu, L.; Zhang, S. D.; Ping, K.; Ni, H. Y.; Qin, X. Y.; Zhao, C. J.; Wang, W.; Efferth, T.; Fu, Y. J. Cryptochlorogenic acid attenuates LPS-induced inflammatory response and oxidative stress via upregulation of the Nrf2/HO-1 signaling pathway in RAW 264.7 macrophages. *Int. Immunopharmacol.* **2020**, *83*, 106436.
(30) Che, D.; Zhao, B.; Fan, Y.; Han, R.; Zhang, C.; Qin, G.; Adams, S.; Jiang, H. Eleutheroside B increase tight junction proteins and anti-inflammatory cytokines expression in intestinal porcine jejunum epithelial cells (IPEC-J2). *J. Anim. Physiol. Anim. Nutr.* **2019**, *103*, 1174−1184.
(31) Weng, Z.; Chi, Y.; Xie, J.; Liu, X.; Hu, J.; Yang, F.; Li, L. Anti-Inflammatory Activity of Dehydroandrographolide by TLR4/NF-κB Signaling Pathway Inhibition in Bile Duct-Ligated Mice. *Cell. Physiol. Biochem.* **2018**, *49*, 1083−1096.
(32) Yu, Z.; Yang, L.; Deng, S.; Liang, M. Daidzein ameliorates LPS-induced hepatocyte injury by inhibiting inflammation and oxidative stress. *Eur. J. Pharmacol.* **2020**, *885*, 173399.
(33) Liu, X.; Zhao, W.; Wang, W.; Lin, S.; Yang, L. Puerarin suppresses LPS-induced breast cancer cell migration, invasion and adhesion by blockage NF-κB and Erk pathway. *Biomed. Pharmacother.* **2017**, *92*, 429−436.
(34) Hien, T. T.; Kim, H. G.; Han, E. H.; Kang, K. W.; Jeong, H. G. Molecular mechanism of suppression of MDR1 by puerarin from Pueraria lobata via NF-kappaB pathway and cAMP-responsive element transcriptional activity-dependent up-regulation of AMP-activated protein kinase in breast cancer MCF-7/adr cells. *Mol. Nutr. Food Res.* **2010**, *54*, 918−928.
(35) Choi, E. J.; Kim, G. H. Daidzein causes cell cycle arrest at the G1 and G2/M phases in human breast cancer MCF-7 and MDA-MB-453 cells. *Phytomedicine* **2008**, *15*, 683−690.
(36) Jin, S.; Zhang, Q. Y.; Kang, X. M.; Wang, J. X.; Zhao, W. H. Daidzein induces MCF-7 breast cancer cell apoptosis via the mitochondrial pathway. *Ann. Oncol.* **2010**, *21*, 263−268.
(37) Bao, C.; Namgung, H.; Lee, J.; Park, H. C.; Ko, J.; Moon, H.; Ko, H. W.; Lee, H. J. Daidzein suppresses tumor necrosis factor-α induced migration and invasion by inhibiting hedgehog/Gli1 signaling in human breast cancer cells. *J. Agric. Food Chem.* **2014**, *62*, 3759−3767.
(38) Guo, J.; Wang, Q.; Zhang, Y.; Sun, W.; Zhang, S.; Li, Y.; Wang, J.; Bao, Y. Functional daidzein enhances the anticancer effect of topotecan and reverses BCRP-mediated drug resistance in breast cancer. *Pharmacol. Res.* **2019**, *147*, 104387.
(39) Lee, C. H.; Huang, C. W.; Chang, P. C.; Shiau, J. P.; Lin, I. P.; Lin, M. Y.; Lai, C. C.; Chen, C. Y. Reactive oxygen species mediate the chemopreventive effects of syringin in breast cancer cells. *Phytomedicine* **2019**, *61*, 152844.
(40) Pfisterer, P. H.; Rollinger, J. M.; Schyschka, L.; Rudy, A.; Vollmar, A. M.; Stuppner, H. Neoandrographolide from Andrographis paniculata as a potential natural chemosensitizer. *Planta Med.* **2010**, *76*, 1698−1700.
(41) Zhang, J.; Sun, Y.; Zhong, L. Y.; Yu, N. N.; Ouyang, L.; Fang, R. D.; Wang, Y.; He, Q. Y. Structure-based discovery of neo-andrographolide as a novel inhibitor of Rab5 to suppress cancer growth. *Comput. Struct. Biotechnol. J.* **2020**, *18*, 3936−3946.
(42) Hsieh, M. J.; Chen, J. C.; Yang, W. E.; Chien, S. Y.; Chen, M. K.; Lo, Y. S.; Hsi, Y. T.; Chuang, Y. C.; Lin, C. C.; Yang, S. F. Dehydroandrographolide inhibits oral cancer cell migration and invasion through NF-κB-, AP-1-, and SP-1-modulated matrix metalloproteinase-2 inhibition. *Biochem. Pharmacol.* **2017**, *130*, 10−20.
(43) Ristimäki, A.; Sivula, A.; Lundin, J.; Lundin, M.; Salminen, T.; Haglund, C.; Joensuu, H.; Isola, J. Prognostic significance of elevated cyclooxygenase-2 expression in breast cancer. *Cancer Res.* **2002**, *62*, 632−635.

https://doi.org/10.1021/acsomega.2c01921
ACS Omega 2022, 7, 28003−28015

(44) Larkins, T. L.; Nowell, M.; Singh, S.; Sanford, G. L. Inhibition of cyclooxygenase-2 decreases breast cancer cell motility, invasion and matrix metalloproteinase expression. *BMC Cancer* **2006**, *6*, 181.
(45) Du, Y.; Shi, A.; Han, B.; Li, S.; Wu, D.; Jia, H.; Zheng, C.; Ren, L.; Fan, Z. COX-2 silencing enhances tamoxifen antitumor activity in breast cancer in vivo and in vitro. *Internet J. Oncol.* **2014**, *44*, 1385−1393.
(46) Majumder, M.; Xin, X.; Liu, L.; Tutunea-Fatan, E.; Rodriguez-Torres, M.; Vincent, K.; Postovit, L. M.; Hess, D.; Lala, P. K. COX-2 Induces Breast Cancer Stem Cells via EP4/PI3K/AKT/NOTCH/WNT Axis. *Stem Cells* **2016**, *34*, 2290−2305.
(47) Hu, J.; Guo, P.; Zhang, Y.; Huang, Z.; Chen, B. MicroRNA-322 regulates the growth, chemosensitivity, migration and invasion of breast cancer cells by targeting NF-kB1. *J. BUON.* **2020 Jan-Feb**, *25*, 152−158.
(48) Glynn, S. A.; Boersma, B. J.; Dorsey, T. H.; Yi, M.; Yfantis, H. G.; Ridnour, L. A.; Martin, D. N.; Switzer, C. H.; Hudson, R. S.; Wink, D. A.; et al. Increased NOS2 predicts poor survival in estrogen receptor-negative breast cancer patients. *J. Clin. Invest.* **2010**, *120*, 3843−3854.
(49) Zhang, J.; Lin, X.; Wu, L.; Huang, J. J.; Jiang, W. Q.; Kipps, T. J.; Zhang, S. Aurora B induces epithelial-mesenchymal transition by stabilizing Snail1 to promote basal-like breast cancer metastasis. *Oncogene* **2020**, *39*, 2550−2567.
(50) Shao, F.; Pang, X.; Baeg, G. H. Targeting the JAK/STAT Signaling Pathway for Breast Cancer. *Curr. Med. Chem.* **2021**, *28*, 5137−5151.
(51) Jang, H.; Ko, H.; Song, K.; Kim, Y. S. A Sesquiterpenoid from Farfarae Flos Induces Apoptosis of MDA-MB-231 Human Breast Cancer Cells through Inhibition of JAK-STAT3 Signaling. *Biomolecules* **2019**, *9*, 278.
(52) Yang, B.; Shen, J. W.; Zhou, D. H.; Zhao, Y. P.; Wang, W. Q.; Zhu, Y.; Zhao, H. J. Precise discovery of a STAT3 inhibitor from Eupatorium lindleyanum and evaluation of its activity of anti-triple-negative breast cancer. *Nat. Prod. Res.* **2019**, *33*, 477−485.
(53) Yang, J.; Chen, L.; Yan, Y.; Qiu, J.; Chen, J.; Song, J.; Rao, Q.; Ben-David, Y.; Li, Y.; Hao, X. BW18, a C-21 steroidal glycoside, exerts an excellent anti-leukemia activity through inducing S phase cell cycle arrest and apoptosis via MAPK pathway in K562 cells. *Biomed. Pharmacother.* **2019**, *112*, 108603.
(54) Fu, S.; Cheng, R.; Xiang, Z.; Deng, Z.; Liu, T. Rapid Profiling of Chemical Constituents in Qingfei Paidu Granules Using High Performance Liquid Chromatography Coupled with Q Exactive Mass Spectrometry. *Chromatographia* **2021**, *84*, 1035−1048.
(55) Ru, J.; Li, P.; Wang, J.; Zhou, W.; Li, B.; Huang, C.; Li, P.; Guo, Z.; Tao, W.; Yang, Y.; et al. TCMSP: a database of systems pharmacology for drug discovery from herbal medicines. *J. Cheminf.* **2014**, *6*, 13.
(56) Chen, C. Y. TCM Database@Taiwan: the world's largest traditional Chinese medicine database for drug screening in silico. *PLoS One* **2011**, *6*, No. e15939.
(57) Xu, H. Y.; Zhang, Y. Q.; Liu, Z. M.; Chen, T.; Lv, C. Y.; Tang, S. H.; Zhang, X. B.; Zhang, W.; Li, Z. Y.; Zhou, R. R.; et al. ETCM: an encyclopaedia of traditional Chinese medicine. *Nucleic Acids Res.* **2019**, *47*, D976−D982.
(58) Wu, Y.; Zhang, F.; Yang, K.; Fang, S.; Bu, D.; Li, H.; Sun, L.; Hu, H.; Gao, K.; Wang, W.; et al. SymMap: an integrative database of traditional Chinese medicine enhanced by symptom mapping. *Nucleic Acids Res.* **2019**, *47*, D1110−D1117.
(59) Xu, X.; Zhang, W.; Huang, C.; Li, Y.; Yu, H.; Wang, Y.; Duan, J.; Ling, Y. A novel chemometric method for the prediction of human oral bioavailability. *Int. J. Mol. Sci.* **2012**, *13*, 6964−6982.
(60) Tao, W.; Xu, X.; Wang, X.; Li, B.; Wang, Y.; Li, Y.; Yang, L. Network pharmacology-based prediction of the active ingredients and potential targets of Chinese herbal Radix Curcumae formula for application to cardiovascular disease. *J. Ethnopharmacol.* **2013**, *145*, 1−10.
(61) Szklarczyk, D.; Santos, A.; von Mering, C.; Jensen, L. J.; Bork, P.; Kuhn, M. STITCH 5: augmenting protein-chemical interaction networks with tissue and affinity data. *Nucleic Acids Res.* **2016**, *44*, D380−D384.
(62) Wishart, D. S.; Feunang, Y. D.; Guo, A. C.; Lo, E. J.; Marcu, A.; Grant, J. R.; Sajed, T.; Johnson, D.; Li, C.; Sayeeda, Z.; et al. DrugBank 5.0: a major update to the DrugBank database for 2018. *Nucleic Acids Res.* **2018**, *46*, D1074−D1082.
(63) Davis, A. P.; Grondin, C. J.; Johnson, R. J.; Sciaky, D.; McMorran, R.; Wiegers, J.; Wiegers, T. C.; Mattingly, C. J. The Comparative Toxicogenomics Database: update 2019. *Nucleic Acids Res.* **2019**, *47*, D948−D954.
(64) Li, Y. H.; Yu, C. Y.; Li, X. X.; Zhang, P.; Tang, J.; Yang, Q.; Fu, T.; Zhang, X.; Cui, X.; Tu, G.; et al. Therapeutic target database update 2018: enriched resource for facilitating bench-to-clinic research of targeted therapeutics. *Nucleic Acids Res.* **2018**, *46*, D1121−D1127.
(65) Pletscher-Frankild, S.; Pallejà, A.; Tsafou, K.; Binder, J. X.; Jensen, L. J. DISEASES: text mining and data integration of disease-gene associations. *Methods* **2015**, *74*, 83−89.
(66) Rappaport, N.; Twik, M.; Plaschkes, I.; Nudel, R.; Iny Stein, T.; Levitt, J.; Gershoni, M.; Morrey, C. P.; Safran, M.; Lancet, D. MalaCards: an amalgamated human disease compendium with diverse clinical and genetic annotation and structured search. *Nucleic Acids Res.* **2017**, *45*, D877−D887.
(67) Shannon, P.; Markiel, A.; Ozier, O.; Baliga, N. S.; Wang, J. T.; Ramage, D.; Amin, N.; Schwikowski, B.; Ideker, T. Cytoscape: a software environment for integrated models of biomolecular interaction networks. *Genome Res.* **2003**, *13*, 2498−2504.
(68) Tripathi, S.; Pohl, M. O.; Zhou, Y.; Rodriguez-Frandsen, A.; Wang, G.; Stein, D. A.; Moulton, H. M.; DeJesus, P.; Che, J.; Mulder, L. C.; et al. Meta- and Orthogonal Integration of Influenza "OMICs" Data Defines a Role for UBR4 in Virus Budding. *Cell Host Microbe* **2015**, *18*, 723−735.
(69) Szklarczyk, D.; Gable, A. L.; Nastou, K. C.; Lyon, D.; Kirsch, R.; Pyysalo, S.; Doncheva, N. T.; Legeay, M.; Fang, T.; Bork, P.; et al. The STRING database in 2021: customizable protein-protein networks, and functional characterization of user-uploaded gene/measurement sets. *Nucleic Acids Res.* **2021**, *49*, D605−D612.
(70) Chin, C. H.; Chen, S. H.; Wu, H. H.; Ho, C. W.; Ko, M. T.; Lin, C. Y. cytoHubba: identifying hub objects and sub-networks from complex interactome. *BMC Syst. Biol.* **2014**, *8*, S11.

https://doi.org/10.1021/acsomega.2c01921
ACS Omega 2022, 7, 28003−28015